SPECTRAL ANALYSIS OF THE PROCESS EMISSION DURING LASER WELDING OF AISI 304 STAINLESS STEEL WITH DISK AND ND:YAG LASER

Paper number 1607

Ali Riza Konuk*, Ronald Aarts, Bert Huis in 't Veld

University of Twente, Laboratory of Mechanical Automation, P.O. Box 217, 7500 AE Enschede, The Netherlands.

Abstract

Optical emissions from the laser welding process can be obtained relatively easy in real-time. Such emissions come from the melt pool, keyhole, or plume during welding. Therefore it is very beneficial to establish a clear relation between characteristics of these emissions and the resulting weld quality or the occurrence of welding defects for any of the laser type currently used in industry. Most commonly used in continuous wave (CW) laser welding applications are the CO_2 laser, Nd:YAG laser, diode, disk and fiber lasers. The disk lasers are relatively new and need to be characterized with respect to the nature of their plasma or plume generation. In this paper, the process emissions during laser welding of AISI 304 stainless steel with disk laser and Nd:YAG laser are compared. Broadband spectral analysis between 200 nm and 1100 nm reveals spectral lines as well as the black body radiation emitted from bead-on-plate welding configuration. The relation between the process emission and weld quality is discussed.

Keywords: Laser welding, disk laser, Nd:YAG laser, plasma spectroscopy, melt pool, keyhole formation, transverse heat input.

Introduction

Nowadays, due to the development of laser sources with an almost ideal beam quality [1] like fiber or disk lasers, new possibilities arise to the high speed welding with low heat input. The high beam quality enables achievement of a laser spot of only a few micrometers or working with a long focusing length while still having a small laser spot [2]. In commercially available disk lasers, a Yb:YAG crystal is used to generate laser light at a wavelength of 1030 nm in the kW range with a high efficiency. Because of the high beam quality, beam delivery with a fiber as small as 50 µm is possible. Moreover, disk lasers are compact in size compared to existing Nd:YAG laser sources and the newer lasers consume less energy [3],[4].

For any laser type, in industry there is a strong demand to verify the quality of laser welded joints, preferably in real-time. However, such a direct measurement of the overall weld quality is not feasible. Instead, sensor systems have been investigated and developed to measure more easily available signals that are related to the welding process dynamics. A large variety of systems use e.g. one or more photodiodes or a camera to observe the optical emissions from the welding process. Results of process monitoring and control obtained for CO_2 and Nd:YAG laser welding in the previous decade are summarized in [5].

Photodiodes and cameras observe typically either a single narrow band or alternatively a broad band of wavelengths. On the other hand, spectrometers can be used to obtain a detailed overview of the spectral content of the emission. Aalderink et al. [6] have performed spectral analysis during Nd:YAG laser welding experiments on AA5182, FeP04 and CuNi90/10. Such spectral analysis may reveal information which is relevant for the process behavior [7], [8].

With the ongoing development of modern high brightness lasers, it is necessary to investigate to what extent previously obtained achievements for e.g. Nd:YAG lasers in welding applications, can be transferred to welding with a disk laser. In this study, results of an investigation of the spectral content of the radiation emerging from the welding process using a "classical" Nd:YAG laser and a "modern"

* E-mail of corresponding author: a.r.konuk@ctw.utwente.nl

disk laser are presented. The spectral content is related to the behavior of the welding process.

Experimental Details

Commercially available AISI304 stainless steel sheets of 1 mm thickness were used in the welding experiments. The chemical composition (in wt%) is presented in Table 1. This material is well suited for laser welding applications.

Figure 1 gives a schematic overview of the welding set-up. Bead-on-plate welding experiments were conducted on the sheets using disk (1 kW Trudisk 1000) and Nd:YAG (4 kW Trumpf THL4006D) laser sources in continuous wave (CW) operation.

A set of experiments with the disk laser was carried out using the maximum output power of 1 kW. The laser beam quality is 2 mm·mrad. The laser is equipped with a 50 µm fiber and the beam is focused on the work piece top surface with a lens having a focal length of 200 mm. The beam diameter was 0.4 mm. A similar set of experiments was done using a Nd:YAG laser with a maximum power of 4 kW and beam quality of 25 mm·mrad. The beam was guided through a 600 µm fiber and was also focused on the work-piece with a lens having a 200 mm focal length (Trumpf BEO70 head). Both of the laser welding heads were manipulated with a Stäubili RX-130 robot (figure 2).

Figure 1 Schematic representation of the experimental setup

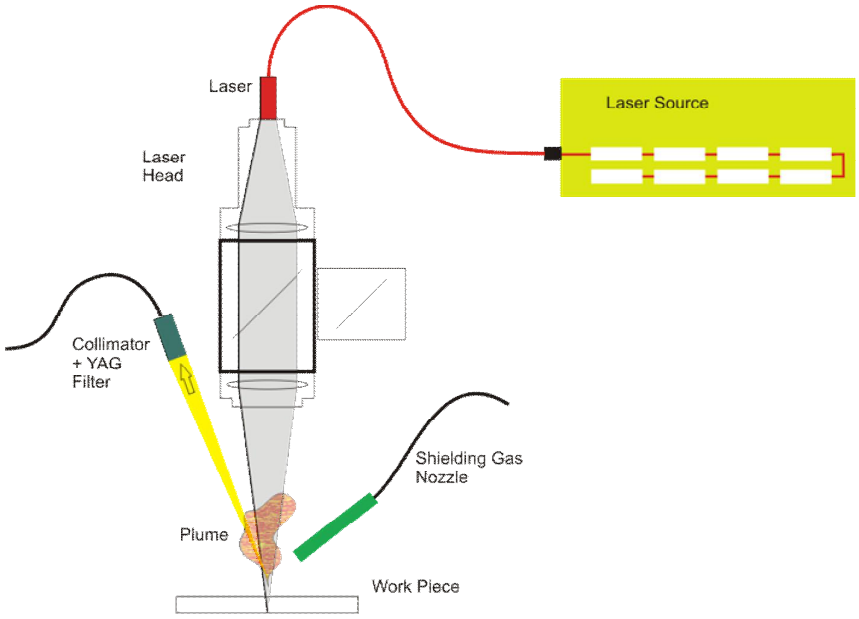

The optical plasma emission was collected with a collimator that was connected to an Ocean Optics spectrometer (HR4000). The quartz collimator had a focal length of 200 mm. The collimator was focused onto the weld pool at an incident angle of 65° as illustrated in figures 1 and 2. An optical filter with a cut-off frequency of 900nm was used to filter 1030 nm and 1064 nm of the disk and Nd:YAG laser radiations, respectively. The collected light was transmitted to a calibrated linear CCD array (200-1100 nm spectral range) by a quartz fiber. The resolution of the spectrometer is 0.25 nm. The signals were analyzed with the spectrometer.

Table 1 Chemical composition (in weight %) of the AISI 304 stainless steel

Element	Weight %
Fe	bal.
Cr	18-20
Ni	8.0 – 10.5
Mn	2.00 max
Si	1.00 max
C	0.08 max
P	0.045 max
S	0.03 max

A special nozzle was used for shielding the weld from oxidation during the solidification process. Argon gas with a maximum flow rate of 400 l/h was used for shielding.

In optical measurements, the spectrometer was used at high speed acquisition mode. The sampling time including acquisition delay was found to be around 5

ms. This results in a maximum sampling rate of 200 Hz. The integration time is adjusted in the range of 100-500 µs according to the emission intensity to avoid saturation.

Several sets of experiments were made with the chosen AISI 304 stainless steel sheets. The welding speed was kept constant and the laser power was varied to observe different welding types such as conduction or keyhole. In order to have a better sampling resolution along the weld, the welding speed was adjusted to 60 mm/s. At this speed, approximately every 0.3 mm on the weld track a spectrum is measured.

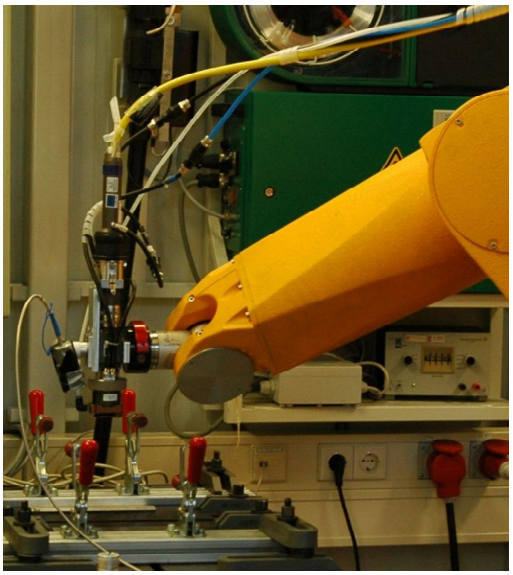

Figure 2 Stäubili RX-130 robotic manipulator with the Trumpf BEO70 laser welding head and the collimator of the spectrometer (on the left)

Results and Discussion

In this section, the intensity distributions of the disk and Nd:YAG lasers are first related to the weld surfaces. Later, the resulting spectral emissions and the transverse cross section microstructure obtained during welding are discussed.

Intensity Distribution

For the lasers used in this work, the laser beam profiles are measured with a Primes diagnostic system. The laser beam intensity profile for the disk and Nd:YAG laser sources are shown in figures 3 and 4.

The main difference between the two laser sources is obvious from these graphs. The intensity of the disk laser spot is concentrated in the center. The overall intensity is more likely to be a Gaussian distribution. The beam diameter is 0.4 mm

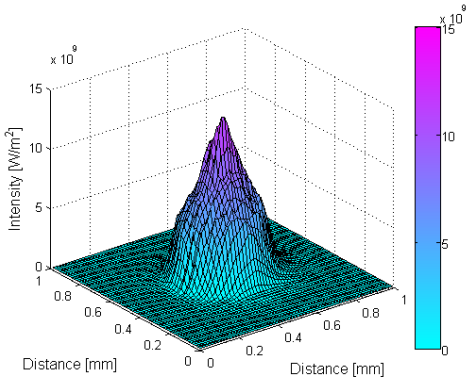

Figure 3 Laser intensity distribution of disk laser at focus (1000W)

The intensity at focus for Nd:YAG laser is more equally distributed than for the disk laser and has a top-hat shape. The beam diameter is 0.6 mm.

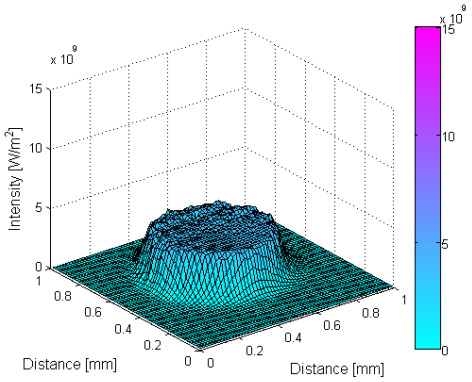

Figure 4 Laser intensity distribution of Nd:YAG laser at focus (1000W)

The effect of the intensity distribution differences between the two types of lasers used on the plasma generation, emission, weld depth and type are considered next.

Transverse Laser Heat Input

Transverse heat input is expected to have an important role on generation of plume and the consequent weld quality. This transverse heat input is defined by integrating the beam intensity over the weld direction *x* and is given by

$$D_t(y) = \int D(x,y)dx \qquad (1)$$

where $D_t(y)$ is the transverse intensity along the welding direction and $D(x,y)$ is the laser power intensity on the surface. The result of integration of focal power intensity along the longitude (x-direction) is given in figure 5. It provides a measure of the input power that is applied at any location in the weld when the transverse cross-section is considered.

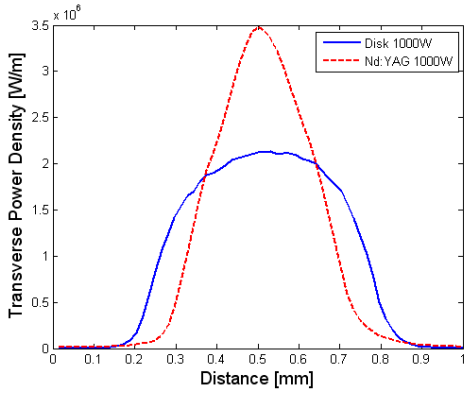

Figure 5 Transverse intensity distribution at laser focal point

Figure 5 shows clearly that the energy absorbed by the work piece will be more concentrated at the center the weld seam, when disk laser is used. With a Nd:YAG laser, the energy will be spread more widely over the track. At the same power, a disk laser would produce much higher temperatures at the weld center than a Nd:YAG laser. This will reflect on the depth of penetration, the keyhole formation and its shape besides plasma generation and the consequent emissions.

Welding Experiments

Several welding experiments with different laser power are made on AISI304 stainless steel. Top and bottom look of the resulting welds are given in figures 6 and 7. In figure 6 the first row shows the surfaces from the disk laser experiments. The Nd:YAG weld surface obtained with the same welding speed and power is compared to the surface produced with the disk laser in the second row.

Creation of the keyhole is more likely with the peaked transverse intensity distribution of disk laser than with the Nd:YAG laser at same amount of power. An observation of the sheet bottom side, (figure 6) shows that 1000W laser power is adequate for full penetration in 1 mm material using the disk laser. The same power level for the Nd:YAG laser results in partial penetration as no weld is visible at the bottom side. The top view of this Nd:YAG weld is uniform and does not show any defect from weld-pool instability. According to figure 7, full penetration starts at 1500W power for Nd:YAG laser. Note that the beam divergence is not taken into consideration as the material thickness is only 1 mm. The deviation of the beam diameter at different depths has, therefore, less effect on the weld process.

These results confirm that, the deeper penetration values for the lasers cannot just be attributed to their power on the work piece. The difference in the transversal power intensity (figure 5) is clearly related to the weld type.

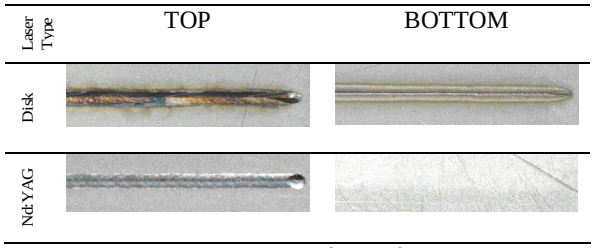

Figure 6 Top and bottom surfaces of weld seams produced by disk and Nd:YAG lasers at 60 mm/s and 1000W laser power (image width 20mm)

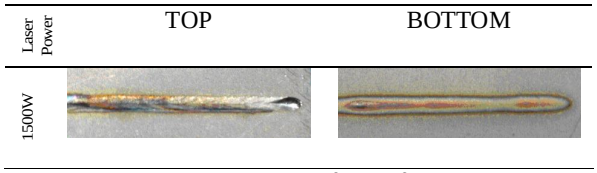

Figure 7 Top and bottom surfaces of weld seam produced by Nd:YAG laser at 60 mm/s and 1500W laser power (image width 20mm)

Transverse Cross Sections

Corresponding cross sections for welds of AISI 304 stainless steel are presented in figures 8 and 9 for disk and Nd:YAG laser welds, respectively. Figure 8 clearly shows that 1000 W is sufficient to obtain full penetration through the samples of 1 mm thickness with the disk laser. The small depth to width ratio of the weld zone in the three cross sections shown in this figure illustrate that keyhole was created during welding.

The cross section of the Nd:YAG laser weld (figure 9) confirms that with 1000 W only a partially penetrated weld is obtained. Moreover, the wide weld bead indicates that a conduction weld has been produced.

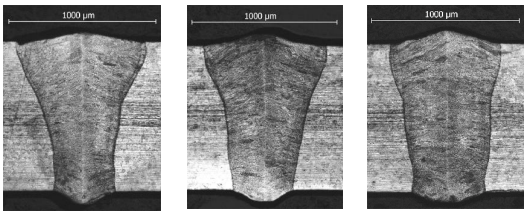

Figure 8 Different transverse cross sections on same track of disk laser welding with varied structure. Speed 60 mm/s, power 1000W

1500W welding - (Keyhole weld)

1000W welding - (Heat Conduction weld)

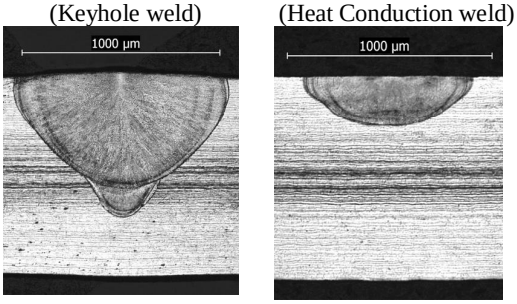

Figure 9 Transverse cross sections of Nd:Yag laser welds. Speed 60 mm/s and varying power

At a power level of 1500 W the onset of the formation of the keyhole is visible. In this particular cross section the penetration is still only partial, but from the bottom view shown in figure 7, it is clear that the penetration depth was varying and full penetration occurred at some locations along the weld. Apparently, at this speed 1500 W power is found to be at the boundary for conduction to keyhole transformation.

Plume and Plasma Generation

From a visual observation of the welding process, it could be concluded that the weld plume and/or plasma are behaving differently for disk and Nd:YAG laser sources. During the experiments with Nd:YAG laser source it is observed that the generation of the plume depends highly on the penetration depth. The more laser power is applied and absorbed by the material, the higher and narrower the plume is. Prior to reaching full penetration depth, the plume becomes unstable and spattering of the molten weld takes place. In many experiments with disk laser the plume and/or plasma induced was also unstable which may be the result of the smaller keyhole.

Spectral Measurements

The emissions of three different welding experiments are summarized in figure 10.

The left column in this figure shows a plot of the spectra that are measured during the complete welding experiment. The spectra have been recorded from 200 to 1100 nm. Hardly any radiation was found in the UV region below 400 nm. In the IR range, the radiation includes the laser light at 1030 or 1064 nm, which was filtered by the optical filter at wavelengths beyond 900 nm. Useful wavelength range is from 400 to 900 nm.

The sample number increases along the other axis of these plots. As was pointed out, the sampling rate is about 200 Hz. It is worthwhile to mention that sampling time (approximately 5 ms) is comparably high to the integration time (100-500 µs). The integration time was adjusted to obtain a high signal level while saturation is avoided. As can be seen in the graphs, some saturation occurred during welding with Nd:YAG laser at 1500 W (sample 420). In future work, the integration time would be dynamically adapted to prevent such saturations.

Thermal Radiation

The broadband background in the spectra of figure 10 is attributed to thermal radiation arising from the high temperatures present in the weld pool, the keyhole and part of the plume. It is related to the well known Planck curve for blackbody radiation that describes the intensity I of the thermal radiation emitted by a hot object with temperature T given by

$$I = e\,I_O = e\,\frac{2p\,hc^2}{l^5}\left(\frac{1}{e^{\frac{hc}{l\,kT}}-1}\right) \qquad (2)$$

In this equation I_O stands for the blackbody radiation emitted as a function of temperature T and wavelength l. For a non-ideal blackbody, the emissivity is e is smaller than one. The constants in the equation are the Planck constant h, the Boltzmann constant k and the speed of the light c. The experimentally observed spectrum cannot be related directly to the Planck curve as the spectrometer is not observing a single well defined temperature. Nevertheless, the large contribution to the spectrum from the broadband black body radiation can be seen clearly in the recorded spectra and the spectral emission lines are superimposed on to this background.

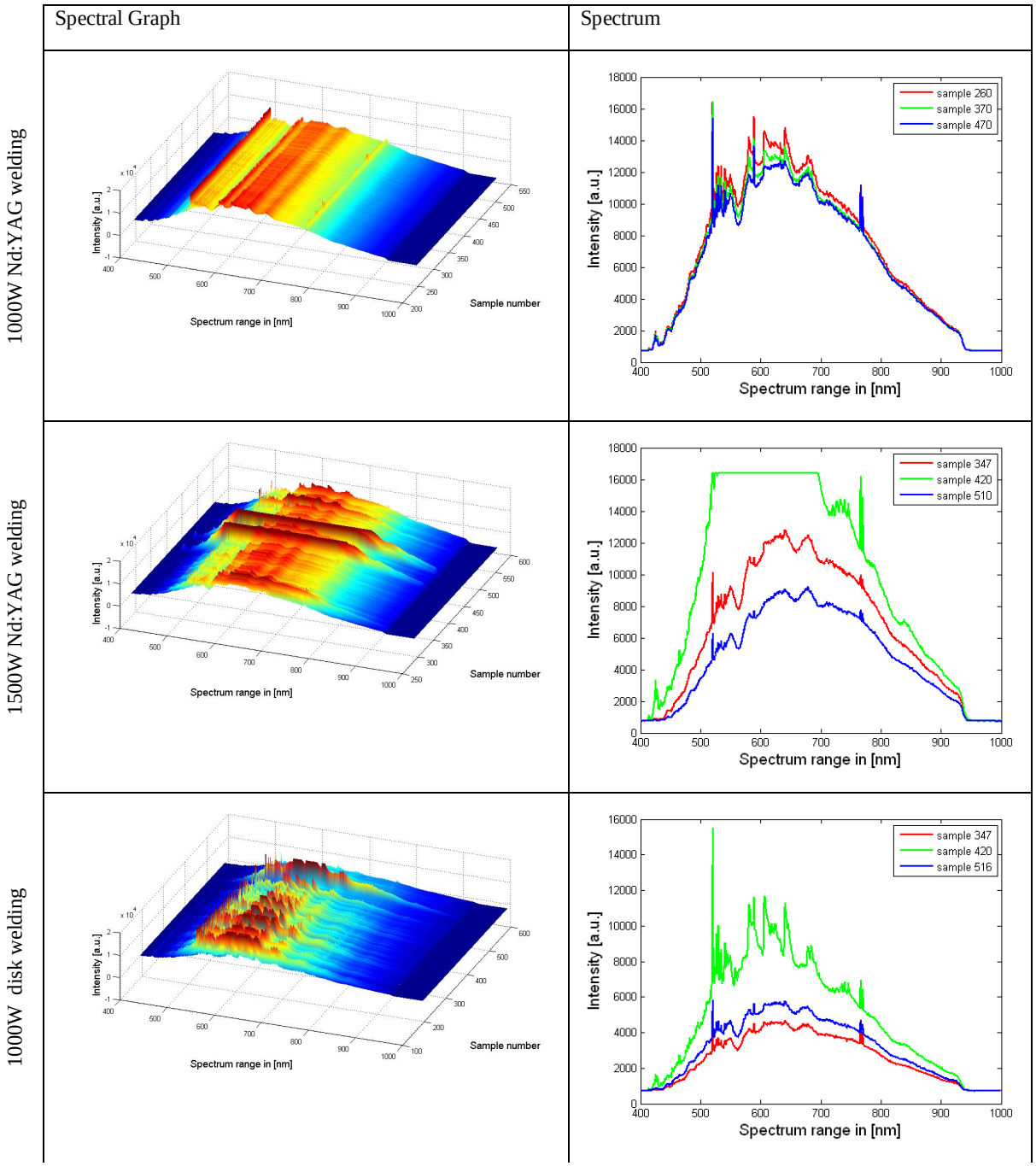

Figure 10 Spectral emission surface plot and selected spectra. Welding speed 60mm/s

Spectral Lines

Peaks in the spectra (figure 10) were compared with the emission lines corresponding to transitions of neutral and singly ionized Fe, Cr, Ni, Mn, O and Ar atoms. The identified spectral lines and their normalized peak height are given in table 3. As the resolution of the spectrometer was only 0.25 nm some of the peaks are combination of two types of atomic or molecular emissions.

The spectral lines are categorized into two types. "active" lines are those with variable intensity during the process. The intensity of the "steady" lines is almost constant. The active lines may be related to the process variations such as weld depth, plume formation. This will be discussed next.

Spectral Emission vs. Process Behavior

The wavelengths of both laser types are 1030 nm and 1064 nm and differ only slightly. It is expected that this small difference hardly affects the spectral emission. On the other hand, the difference in intensity profile (figures 3 and 4) or transverse intensity distribution (figure 5) is significant and has an influence on the process behavior.

Welding with 1000W Nd:YAG source results a smooth surface plot due to the stability of the conduction weld, figure 6. Different spectral samples taken from the surface plot in the upper row of figure 10 reveal that the spectrum is quite steady and that there are not abrupt changes during the weld. Clearly the smooth (conduction) weld appearance results in rather constant spectral emission.

Applying the same power with the disk laser was found to produce a keyhole and a more fluctuating welding process. This behavior is also apparent from the lower row in figure 10. Differences can both be found in the height of the background radiation as well as in the spectral lines. The average absolute height of the background radiation is lower than was found for the Nd:YAG laser. As a large part of this thermal radiation is attributed to the weld pool, the lower intensity is likely to be caused by the smaller weld pool induced by the disk laser.

In the Nd:YAG welds with 1500 W laser power also keyhole is created, although the weld type and penetration depth was not constant along the complete weld seam (figures 7 and 9). Consequently, fluctuating spectra are found as well, middle row figure 10. In some samples the intensity was so high that saturation occurred. Yet it can be observed that the mean intensity of the other spectra is almost identical to the intensity found at 1000 W. This may seem to be in contrast to the observation that during the keyhole welds with 1500 W a much larger plume was present. As was outlined previously, the collimator is focused on the work piece surface and mainly collects emissions from the keyhole, weld pool and the lower part of the plume. Hence, large variations in the height of the plume do not lead to proportional changes in the measured intensity.

Table 3 Identified peaks in the spectra for disk and Nd:YAG laser at 1000W power [9]

Element	Wavelength (nm)	Disk laser		Nd:YAG	
		Steady intensity	Active	Steady intensity	Active
Cr(I)	519,9 - 520,7	11745	+++++	15838	+++
Cr(I)	521,0				+++
Fe(I)	526,7	6587	++		
Fe(III), Cr(I)	529,8	6784	++		++
Cr(I), O(II)	534,4				++
Fe(I), Ni(IV)	580,8 - 581,0		++		++
Ar(I)	589,0			13967	++
Fe(III), Ni(I)	589,2	7275	+++		
Fe(I)	591,3		++		
Fe(I)	606,6	6813	++		++
Fe(I)	607,9	6643			
O(IV)	609,2		++		
Fe(III)	618,6			13089	
Mn (IV)	623,5		++		
Mn (III)	623,7			13108	
Ni (XVII)	626,8			13082	
Mn(V)	632,9		+	13281	
Ni(I), Fe(II)	640,3 - 640,8	6648	++	13379	
Fe(I)	641,1 - 641,3	6682			
Fe(I)	642,1	6563		13206	
Cr(IV), Fe(II)	766,4				+++++
Fe(III)	769,9				+++

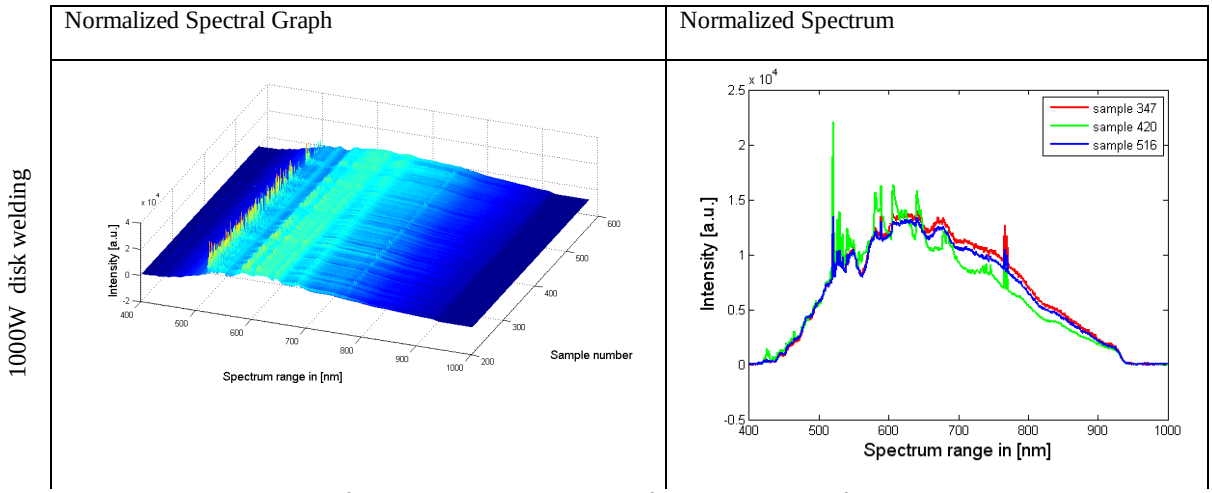

Figure 11 Spectral emission surface plot and selected spectra after normalization of the disk laser welding experiment shown in figure 10. Welding speed 60mm/s

Normalization

Comparing the spectral lines in the emissions from disk and Nd:YAG welds is not straightforward as the intensities are fluctuating in the spectra from the disk laser welds. Therefore a normalization procedure is proposed to minimize the overall intensity variation of the spectra in each measurement set. During this normalization, the average intensities at two selected wavelengths are computed and next all spectra are scaled to set the intensities at these wavelength close to their mean values. A mathematical expression for the normalized intensity $I_n(t,\lambda)$ is

$$I_n(t, l) = \frac{\left(\frac{I(t, l_1)}{\bar{I}(l_1)} + \frac{I(t, l_2)}{\bar{I}(l_2)} \right)}{2} \qquad (3)$$

where the average intensities at wavelength λ_1 is

$$\bar{I}(l_1) = \frac{1}{n} . \sum_{t=1}^{n} I(t, l_1) \qquad (4)$$

and an analogous expression at wavelength λ_2 is applied. In the equation λ represents the wavelength and t stands for the sample number.

For the normalization two wavelengths are selected at which no spectral lines are found. For AISI304 506 and 555 nm appear to be useful. Selection of some other pair could be possible for an optimum solution. The resulting normalized spectrum of the disk laser experiment is given in figure 11. It shows that the level of the background thermal radiation has become almost constant after normalization. The intensity of the spectral lines is still fluctuating significantly. The relation between the measured intensities and the process behaviour will be investigated in the future.

From a comparison of the normalized disk laser spectrum (figure 11) with the spectrum of the Nd:YAG laser experiment (upper row of figure 10), it appears that different spectral lines are observed. More specifically, the weld pool emission spectra for the two different laser sources are different at the range of 600-650 nm as can also be seen in the overview of table 3. It implies that there is no guarantee that an analysis of the spectral lines in relation to the process behavior carried out for one laser type, can be applied to another laser without modification. A spectrometer with a sufficiently large wavelength range can measure all relevant spectral lines and may be useful for either laser type.

Conclusions

Spectrometric measurements were made from welding experiments on 1 mm AISI 304 with the disk and the Nd:YAG lasers with same speed and varying laser power levels. The spectral data, weld surface appearance and transverse cross-sections obtained with these two laser sources are compared to each

other. Also the spectral lines of the spectra are identified.

The spectral measurements reveal that there is very less UV light emitted during disk and Nd:YAG laser welding of AISI304. An optical filter blocks wavelengths beyond 900 nm to avoid exposure of the spectrometer to the laser radiation at 1030 nm or 1064 nm. Hence, the emission range considered in this paper is in between 400 and 900 nm.

The transverse cross-sections of 1000W Nd:YAG welding show the weld to be a conduction type. However, for the same power and speed, the weld type is clearly keyhole for the disk laser. This difference in weld type can be attributed to the different intensity distributions of the lasers used. During keyhole welding it is observed that the process is much more fluctuating than in the case of conduction welding. In this case the measured intensity of the spectral emissions is rather unstable for disk laser welding at 1000 W, whereas almost constant spectra are recorded during Nd:YAG laser welding at this power. At a higher power level, also the emissions from the Nd:YAG laser welding become more unsteady.

In order to better characterize the spectral content, a normalization procedure is proposed. The normalization of the spectrometric data should be done by selecting the least active wavelengths, i.e. wavelengths where no spectral lines are present. These normalization wavelengths depend on the material type and do not change with the type of the laser source. This normalization method will be investigated in the future to monitor weld quality.

The applied off-axis placement of the spectrometer collimator is considered to be beneficial. It is focused on the surface of the work piece such that the contribution from the fluctuating plume to the recorded spectra is reduced.

Real-time spectral measurements are important since they give more information than broadband optical sensors using photodiodes. Their biggest advantage is that they can easily be adapted to the considered wavelengths with respect to any welding process. This means that there is no need to replace the overall system when changing the material and/or laser. However, a drawback of systems based on spectral emissions is that they are relatively slow compared to systems with optical sensors.

References

[1] Weberpals, J. and Dausinger, F. and Göbel, G. & Brenner, B. (2007), Role of strong focusability on the welding process, Journal of laser applications, 252-258.

[2] Kim C., Kim J., Lim H. & Kim J. (2008), Investigation of laser remote welding using disc laser, Journal of Materials Processing Technology, 521 – 525.

[3] Contag K., Karszewski M., Stewen C., Giesen A. and Hugel H. (1999), Theoretical modelling and experimental investigations of the diode-pumped thin-disk Yb : YAG laser, Quantum Electronics, 697.

[4] Ahmed, N. (2005) New Developments in Advanced Welding. Woodhead Publishing, Cambridge.

[5] Duley, W.W. (1999) Laser Welding, John Wiley and Sons, Inc.

[6] Aalderink, B.J., Aarts, R.G.K.M. & Jonker, J.B. Meijer, J. (2005), Weld Plume Emissions During Nd:YAG Laser Welding, Proceedings of the third International WLT-conference on Laser in Manufacturing, 413-417.

[7] Sibillano T., Ancona A., Berardi V. & Lugarà P.M. (2009), A Real-Time Spectroscopic Sensor for Monitoring Laser Welding Processes, Sensors, 3376-3385.

[8] Sibillano T., Ancona A., Lugarà P. M., Miric M., (2009), Discrete wavelet analysis of the optical emission during CO_2 laser welding of stainless steel, Proceedings of the Fifth International WLT-Conference on Lasers in Manufacturing, pages 381-385.

[9] National Institute of Standards and Technology database (http://physics.nist.gov/PhysRefData/ASD/lines_form.html).

Acknowledgements

This research is carried out under the contract number FP7-SME-2007-1-222279 in the seventh-frame work EU project CLET. The effort of TRUMPF Nederland B.V. to arrange the availability of the TruDisk 1000 disk laser for experiments is appreciated.

Authors would like to acknowledge Dr. Pathiraj for his contributions to the micro-structural analysis and discussions on the paper. For discussions on intensity distributions J.T. Hofman (M2i) is acknowledged. We would also like to sincerely express our thanks to F. Ploegman (LAC) and W. Tax (LAC) for their assistance during the experiments.

Meet the Authors

Ali Riza Konuk is a PhD researcher working at Mechanical Automation group of the University of Twente, Netherlands. He holds an M.Sc. in mechatronics and his main interests lie in the fields of system and control engineering, robotics and laser welding technology.

Ronald Aarts is associate professor in the Mechanical Automation group of the University of Twente, Netherlands. He is working on process and motion control for robotized laser welding.

Prof. Bert Huis in ‘t Veld is a full professor, leading the Chair of Applied Laser Technology of the University of Twente, and also works at TNO (the Netherlands Organisation for Applied Scientific Research) in Eindhoven, in the Netherlands.